

See discussions, stats, and author profiles for this publication at: <https://www.researchgate.net/publication/256488743>

# Particle Shape Anisotropy in Pickering Emulsions: Cubes and Peanuts

ARTICLE *in* LANGMUIR · SEPTEMBER 2013

Impact Factor: 4.46 · DOI: 10.1021/la402427q · Source: PubMed

---

CITATIONS

11

READS

34

## 6 AUTHORS, INCLUDING:



Eline M. Hutter

Delft University of Technology

7 PUBLICATIONS 22 CITATIONS

[SEE PROFILE](#)



Sonja I R Castillo

Utrecht University

7 PUBLICATIONS 133 CITATIONS

[SEE PROFILE](#)



Albert P Philipse

Utrecht University

189 PUBLICATIONS 6,465 CITATIONS

[SEE PROFILE](#)



Willem K Kegel

Utrecht University

72 PUBLICATIONS 1,699 CITATIONS

[SEE PROFILE](#)

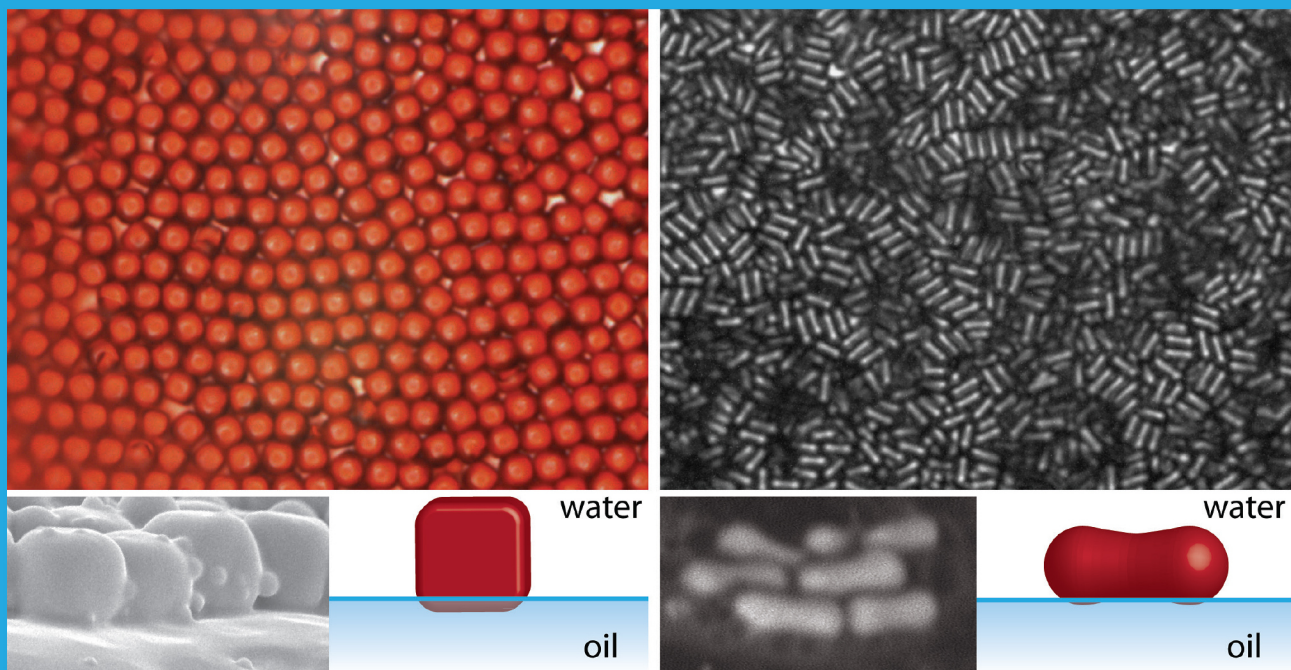
# Langmuir

The ACS Journal of Surfaces and Colloids

FEBRUARY 4, 2014

VOLUME 30, NUMBER 4

[pubs.acs.org/Langmuir](http://pubs.acs.org/Langmuir)



## Particle Shape Anisotropy in Pickering Emulsions: Cubes and Peanuts

(see p. 5A)



ACS Publications

MOST TRUSTED. MOST CITED. MOST READ.

[www.acs.org](http://www.acs.org)

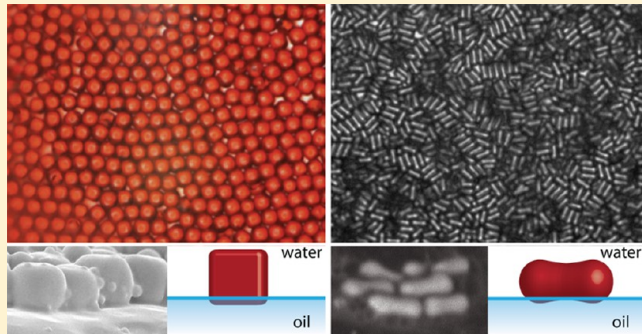
## Particle Shape Anisotropy in Pickering Emulsions: Cubes and Peanuts

Julius W. J. de Folter,\* Eline M. Hutter, Sonja I. R. Castillo, Kira E. Klop, Albert P. Philipse, and Willem K. Kegel\*

Van't Hoff Laboratory for Physical and Colloid Chemistry, Debye Institute for NanoMaterials Science, Utrecht University, Padualaan 8, Utrecht, The Netherlands

### Supporting Information

**ABSTRACT:** We have investigated the effect of particle shape in Pickering emulsions by employing, for the first time, cubic and peanut-shaped particles. The interfacial packing and orientation of anisotropic microparticles are revealed at the single-particle level by direct microscopy observations. The uniform anisotropic hematite microparticles adsorb irreversibly at the oil–water interface in monolayers and form solid-stabilized o/w emulsions via the process of limited coalescence. Emulsions were stable against further coalescence for at least 1 year. We found that cubes assembled at the interface in monolayers with a packing intermediate between hexagonal and cubic and average packing densities of up to 90%. Local domains displayed densities even higher than theoretically achievable for spheres. Cubes exclusively orient parallel with one of their flat sides at the oil–water interface, whereas peanuts preferentially attach parallel with their long side. Those peanut-shaped microparticles assemble in locally ordered, interfacial particle stacks that may interlock. Indications for long-range capillary interactions were not found, and we hypothesize that this is related to the observed stable orientations of cubes and peanuts that marginalize deformations of the interface.



### INTRODUCTION

The first clear description of solid particles acting as stabilizers of fluid–fluid interfaces can be found in the seminal, century-old work of Ramsden in 1903<sup>1</sup> and Pickering in 1907.<sup>2</sup> The recent resurgence of Ramsden–Pickering emulsions and foams is driven by the stimulating combination of industrial applicability and fundamental scientific interest. Interfacial particle adsorption is, for instance, widely employed in food, cosmetic, and pharmaceutical applications and plays a pivotal role in froth flotation, which is relevant for oil recovery and metallurgical refining. Solid particles may also be used as environmentally friendly alternatives for commonly used surfactants.

To date, many factors influencing the formation and stability of solid-stabilized emulsions have been investigated. For instance, different materials have been employed for emulsion stabilization, including silica, polystyrene, Teflon, iron oxide, metal sulfate, and clay particles.<sup>3</sup> In a number of studies, the use of particles from naturally available materials was explored.<sup>4–6</sup> Particle size<sup>7</sup> and wettability<sup>8</sup> are important parameters governing the stabilization of Pickering emulsions, which may also form spontaneously<sup>9–11</sup> and can be controlled by external stimuli such as pH,<sup>12–14</sup> temperature,<sup>15,16</sup> and magnetic fields.<sup>17</sup>

For efficient emulsion stabilization, particles need to be partially wettable by both the oil and water phases. Upon

mixing of oil, water, and solid particles, the latter adsorb irreversibly at the oil–water interface. Initially, the interfacial particle coverage is insufficient to halt droplet coalescence. As droplets grow in size, the degree of particle coverage increases until a dense interfacial particle layer is formed that inhibits further coalescence. This process is known as limited coalescence<sup>18–21</sup> and generates kinetically stable emulsions with relatively narrow droplet size distributions. More than half a century ago, in 1954, Wiley reported the first systematic study dedicated to limited coalescence in emulsions.<sup>19</sup> He derived expressions underlying the limited coalescence of oil droplets in the presence of emulsifier particles. Interestingly, it was assumed that the interface was covered with a close-packed monolayer of cubes. With this study, we provide the first experimental realization of Wiley's prototypical model system using particles with a cubic shape.

This is in contrast to most Pickering emulsion studies, where spherical particles are used as solid stabilizers. Recently, the interfacial behavior of particles with anisotropic shapes has received widespread attention. The increasing availability of anisotropic particles offers the possibility to study their

Received: June 27, 2013

Revised: September 10, 2013

Published: September 11, 2013

influence on particle interactions at the interface, their orientations and packing densities, and their effect on emulsion and foam stability. However, anisotropic particles that have been used to study the Pickering-type stabilization of fluid interfaces are often polydisperse.<sup>22–25</sup> A limited number of systems exploiting the interfacial self-assembly of monodisperse, anisotropic particles have been investigated, including millimeter-scale objects with complex shapes,<sup>26</sup> sharp-tipped ellipsoids,<sup>27–32</sup> and cylinders<sup>33,34</sup> that may induce long-range attractive capillary interactions.

Here we study particle shape anisotropy in Pickering emulsions by employing, for the first time, particles with well-defined cubic and peanut-type shapes.<sup>35–38</sup> We investigate the packing and orientation of the anisotropic microparticles at the oil–water interface on the single-particle level. The most important energy contribution opposing emulsion stability is the fraction of the residual bare oil–water interface. Previously, Pickering emulsions have been stabilized with varying particle coverage, ranging from poorly protected interfaces to the densest sphere packings.<sup>14</sup> Therefore, it is of conceptual interest to push the particle coverage to a maximum and the energetically costly residual oil–water interface to a minimum. We have pursued this fundamental challenge by demonstrating that cubes allow for an interfacial coverage that exceeds the densest packing of spheres. Moreover, we reveal that the cubes and peanuts all display an exclusive interfacial orientation.

## EXPERIMENTAL SECTION

**Materials.** Iron(III) chloride hexahydrate (ACS reagent, puriss. p.a., 98.0–102%), decane ( $\geq 99\%$ ), styrene, *n*-dodecane ( $> 99\%$ ), hexadecane, and isopropylmyristate (98%) were obtained from Sigma-Aldrich. Sodium sulfate (anhydrous, 99%), 2,2'-azobis(2-methylpropionitrile) (AIBN, 98%), *n*-octane ( $> 99\%$ ), tetradecone (99%), and methyloctanoate (99%) were purchased from Acros. Sodium hydroxide pellets were obtained from Merck, and hydroquinone ( $\geq 99\%$ ) was obtained from Riedel-de Haën. All chemicals were used as received. Water used in all experiments was purified by filtration through Millipore filters.

**Synthesis of Hematite Cubes, Ellipsoids, and Peanuts.** Uniform cubic hematite ( $\alpha$ -Fe<sub>2</sub>O<sub>3</sub>) microparticles were prepared following Sugimoto's gel–sol method.<sup>35</sup> In a typical synthesis, 100 mL of 5.4 M NaOH was slowly added in approximately 5 min to 100 mL of a magnetically stirred 2.0 M FeCl<sub>3</sub> solution. Subsequently, the obtained condensed iron hydroxide gel was aged at 100 °C for 8 days. The resulting precipitated particles were then purified by 3-fold centrifugation and redispersion in 200 mL of Millipore water. Cubes of different sizes were synthesized by varying the excess concentration of Fe<sup>3+</sup> ions relative to that of hydroxide ions,<sup>35,39</sup> their size increasing with [Fe<sup>3+</sup>]. To modify the morphology of the hematite microparticles from cubic to ellipsoidal or peanut-shaped, sulfate ions were introduced.<sup>36</sup> The preparation of ellipsoids and peanuts was similar to the procedure for the cubes except that 90 mL of 6.0 M NaOH and 10 mL of 0.82 or 0.25 M sodium sulfate were added to the ferric hydroxide gel, respectively. Sulfate ions strongly adsorb to hematite faces parallel to the (long) *c* axis, inhibiting particle growth in the direction normal to the *c* axis.<sup>40</sup>

**Emulsion Preparation.** Emulsions with varying concentrations of hematite microparticles, expressed in weight percentage (wt %), were prepared. To this end, aqueous hematite dispersions were sonicated in an ultrasonic bath for 30 min prior to emulsification to ensure that particles were well dispersed. Next, desired amounts of aqueous dispersions with known particle concentrations were added to glass vials and, if necessary, were adjusted with Millipore water to a volume of 2 mL. The particle concentrations mentioned are all based on this aqueous phase of the emulsions. Typically, 2 mL of oil was added and oil-in-water emulsions were formed by vigorous manual shaking for at least 1 min. Hence, emulsions were prepared in a 1:1 volume ratio

with a total volume of 4 mL. After emulsification, samples were allowed to equilibrate over time through limited coalescence to reach their final droplet size distribution. For most emulsions, decane was used as the oil phase. However, to enable SEM imaging of microparticles at the oil–water interface styrene-in-water emulsions were prepared and solidified by polymerization of the styrene droplets. To inhibit the initiation of polymerization from the water phase, 10 μL of an aqueous 9 mM hydroquinone solution was added. The styrene phase contained 37 mM AIBN, acting as a radical polymerization initiator. Once generated, emulsions were polymerized in an oil bath for 24 h at a temperature of 80 °C.

**Characterization.** *Optical Microscopy.* To study the packing of hematite microparticles at the interface of emulsion droplets, emulsion samples were imaged with a Nikon Eclipse Ti inverse optical microscope. The microscope was equipped with 20×, extra-long working distance 40×, and oil-immersion 100× Nikon objectives. Images were taken with a Lumenera InfinityX CCD camera. To enable visualization, drops of emulsion samples were gently added to a macroscopic aqueous phase and placed on microscope cover slides, which were capped with a closed glass cylinder to prevent evaporation.

*Transmission Electron Microscopy.* The size and shape of the synthesized particles were analyzed by taking transmission electron microscopy (TEM) photographs using a Philips Tecnai 12 microscope operating at an acceleration voltage of 120 kV. Average particle dimensions with standard deviations were determined on the basis of measurements of at least 100 particles with SIS iTEM image analysis software. For each sample, a drop of a diluted dispersion was placed on a Formvar-coated copper grid sputter-coated with carbon.

*Scanning Electron Microscopy.* To observe the arrangement and orientation of the anisotropic hematite microparticles at the oil–water interface, particle-covered styrene emulsion droplets were polymerized and examined with scanning electron microscopy (SEM). Samples were studied with a Philips XLFEIG30 or an FEI Phenom scanning electron microscope. Individual solidified polystyrene droplets were glued to a copper grid with conducting carbon paste. Prior to SEM inspection, samples were sputter-coated with a 8–12-nm-thick platinum layer.

*Contact Angle Measurements.* Three-phase contact angles  $\theta_{ow}$  among oil, water, and hematite were measured with a DataPhysics OCA15 setup. To determine  $\theta_{ow}$ , a polished hematite surface was placed in a continuous oil phase. Then, small ( $\sim 1 \mu\text{L}$ ) water droplets were formed in the oil phase at the tip of a needle and brought into contact with the hematite surface. Subsequently, the needle was gently retracted, leaving behind a water droplet at the hematite surface. Three-phase contact angles were determined automatically, approximating the contour of the imaged droplets with a Laplace–Young fit. Measurements were averaged over eight droplets.

*Droplet Size Measurements.* Average oil droplet diameters were measured for various Pickering emulsion concentration series. Because droplets were visible to the naked eye, droplet sizes could be determined from photographs taken after at least 1 day of equilibration. Emulsions had reached a stable droplet size distribution through limited coalescence. For each emulsion, up to 200 droplets were measured with SIS iTEM image analysis software to determine their surface-weighted average droplet diameter  $D$ ,<sup>21</sup> which is defined as

$$D = \frac{\sum_i n_i D_i^3}{\sum_i n_i D_i^2} \quad (1)$$

with  $n_i$  being the number of droplets with diameter  $D_i$ .

## RESULTS AND DISCUSSION

**Pickering Emulsions with Cubic Microparticles.** *Macroscopic Properties.* Solid-stabilized o/w emulsions were prepared by mixing oil, water, and hematite microparticles with varying sizes and shapes. In contrast to many other solid stabilizers, hematite ( $\alpha$ -Fe<sub>2</sub>O<sub>3</sub>) microparticles displayed intrinsic surface activity in which no additional surface

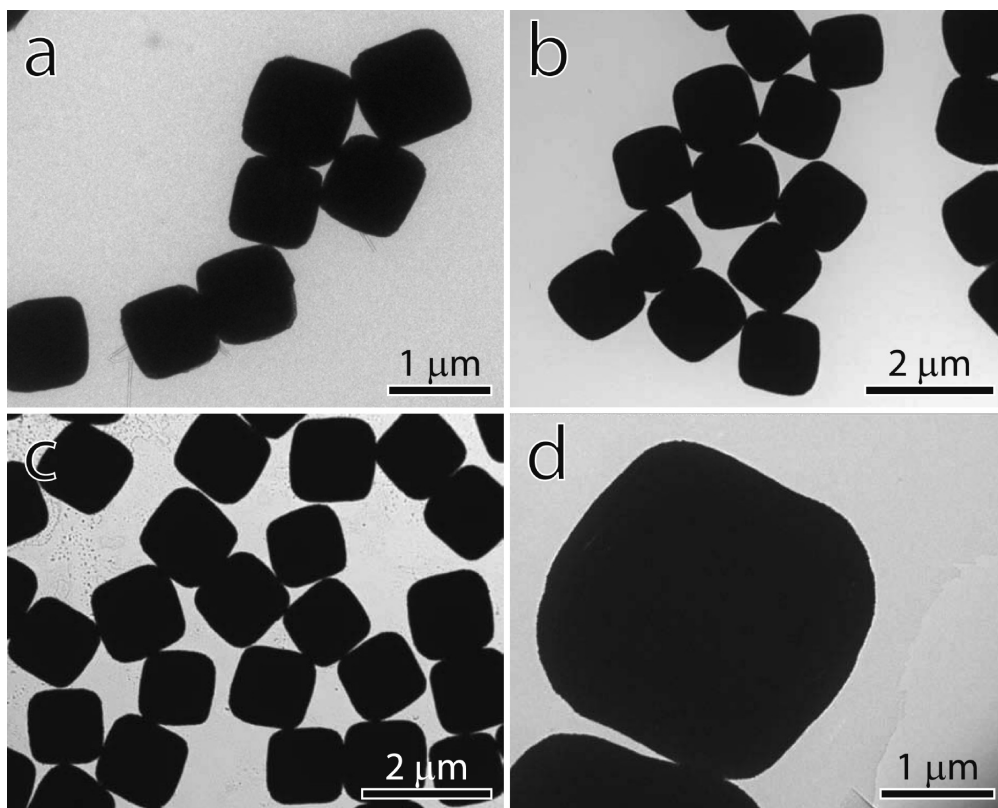


**Figure 1.** Transmission electron microscopy pictures of cubic hematite microparticles with mean side lengths  $d$  of (a)  $0.85 \pm 0.11$ , (b)  $1.27 \pm 0.06$ , (c)  $1.29 \pm 0.09$ , and (d)  $2.64 \pm 0.13 \mu\text{m}$ .

modification or chemical pretreatment was required for their adsorption at the interface. Emulsions were usually prepared with decane or styrene as the oil phase. Nevertheless, stable Pickering emulsions were also obtained with alkanes with different carbon chain lengths (8–16) and esters (methyl octanoate and isopropyl myristate). After emulsification, equilibrated emulsions remained very stable against further coalescence into two macroscopic phases. The process of limited coalescence is followed in time for two samples with different concentrations of cubic microparticles (SI Figure 1 and Video 1). No excess oil phase was observed because the total oil volume was found inside the droplets. Emulsions displayed stable droplet size distributions upon storage for at least more than a year. It was also possible to shake equilibrated emulsions and restart the limited coalescence process with a reproducible droplet size distribution.

To date, cubic particles have not been used to stabilize emulsions. We synthesized uniform hematite cubes with different sizes, as shown in Figure 1, with mean side lengths  $d$  varying from  $0.85$  to  $2.64 \mu\text{m}$ . Because the cubes exhibit rounded edges, their shape closely resembles a superellipsoid, which is described by  $(x/a)^m + (y/a)^m + (z/a)^m = 1$ . Superellipsoids undergo a shape deformation from a sphere to a perfect cube upon changing the shape parameter  $m$  from 2 to infinity.<sup>41</sup> The rounded-edged cubes we used in our experiments exhibited intermediate  $m$  values of between 3.5 and 4, as estimated from superellipsoidal fits to the particle contours.<sup>37</sup> The stabilization of emulsions succeeded for cubic microparticles regardless of their size. Figure 2a shows an emulsion series with different concentrations of stabilizing hematite cubes with  $d = 0.85 \mu\text{m}$ . With this series, we confirm the expected decrease in droplet size with the concentration of

added solid particles. If only numbers amounts of microparticles are present, for instance, 0.4 wt %, then the total interfacial area that can be covered is limited and very large oil droplets with diameters approaching the centimeter range are obtained. The solid content in these samples is just sufficient to prevent full macroscopic phase separation. In contrast, at higher particle concentration a maximum concentration exists beyond which droplets do not become smaller anymore. This depends, for instance, on the intensity of the applied shear in creating the emulsions, which sets the size of the initially generated droplets. Because we use relatively large, heavy particles ( $\rho_{\text{Fe}_2\text{O}_3} \approx 5.2 \text{ g cm}^{-3}$ ), their gravitational length  $L_g = ((kT)/(\Delta mg))$  is much smaller than their own mean side length ( $\ll 10^{-3}d$ ). Despite some inevitable sedimentation of a small fraction of microparticles to the bottom of the vessel, even large cubes with  $d = 2.64 \mu\text{m}$  acted as efficient particle stabilizers of emulsions, as shown for three emulsion samples in Figure 2b. From left to right, the particle concentration increases and the average oil droplet diameter concomitantly decreases.

Because the hematite microparticles are magnetic, we tested their response to the application of a magnetic field using a NdFeB magnet of 1.33 T. The fraction of microparticles that was not adsorbed at the oil–water interface but had sedimented to the bottom of the vessel was attracted by the applied magnetic field. However, the emulsion droplets fully covered by magnetic hematite microparticles showed no response to the magnetic field, irrespective of the particle concentration, size, and shape. This is in contrast to Pickering emulsions stabilized by much more magnetic superparamagnetic iron particles<sup>17</sup> that can even undergo macroscopic phase separation upon application of an external magnetic field with similar strength.

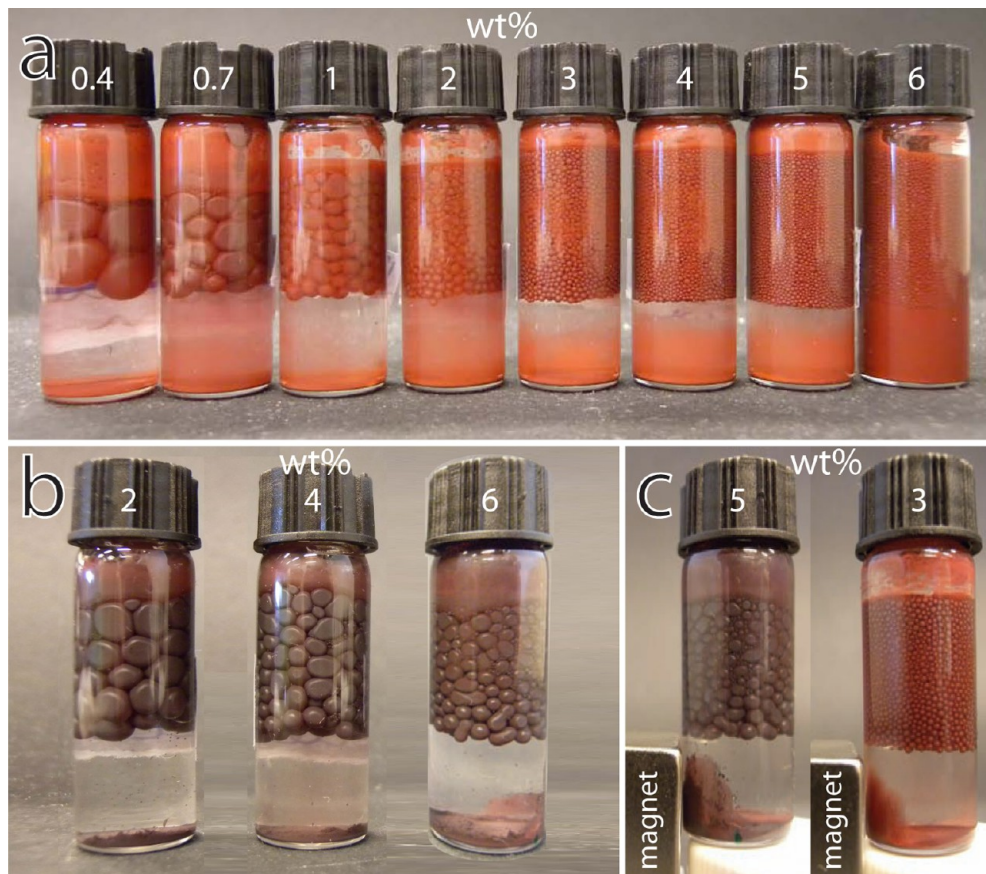


**Figure 2.** Concentration series of Pickering emulsions, containing 2 mL of decane and 2 mL of an aqueous dispersion, stabilized by cubic hematite microparticles with mean side lengths  $d$  of (a) 0.85 and (b) 2.64  $\mu\text{m}$ . (c) Magnetic field applied to emulsions containing cubes with  $d = 2.64$  and 0.85  $\mu\text{m}$ , respectively.

The particles are trapped in a deep energy well that strongly binds them at the interface. For our hematite microparticles, however, the energy associated with interfacial attachment is much higher ( $\sim 10^7 kT$ ) than the magnetic force experienced by the particles. Hence, particle detachment from the interface did not occur. In addition, the dense packing of interfacial monolayers of microparticles does not allow rearrangements such that magnetic moments align with the applied field.

Wiley derived expressions underlying the limited coalescence of oil droplets in the presence of emulsifier particles, relating the droplet size to the amount and size of adsorbed solid particles and the volume of the emulsified phase.<sup>19</sup> Interestingly, it was assumed that the interface was covered with a close-packed monolayer of cubes. For a derivation of the equations, analogous to Wiley, see the Supporting Information. With this study we provide the first experimental realization of Wiley's prototypical model system employing particles with a cubic shape. We have measured the surface-weighted average oil droplet diameter  $D$  in emulsions stabilized by cubic microparticles. Figure 3a plots the inverse average droplet diameter  $D^{-1}$  against the weight percentage (wt %) of hematite cubes for different mean side lengths  $d$ . We verified a linear relationship between  $D^{-1}$  and the wt % of added particles, as expected for limited coalescence in solid-stabilized emulsions.<sup>21</sup> It also corresponds to the equations derived for cubic particles

$$D = \frac{6d\rho_p V_{\text{oil}} C}{m_p^{\text{tot}}} = \frac{6d\rho_p V_{\text{oil}} C}{N_p m_p} \quad (2)$$

where  $D$  is the emulsion droplet diameter,  $d$  is the mean side length of the cubes,  $\rho_p$  is the density of the hematite particles ( $\rho_{\text{Fe}_2\text{O}_3} = 5.2 \text{ g cm}^{-3}$ ),  $V_{\text{oil}}$  is the total oil volume,  $C$  is the interfacial coverage,  $m_p^{\text{tot}}$  is the total mass of adsorbed particles,  $N_p$  is the number of particles adsorbed at the interface, and  $m_p$  is the mass per particle. The slopes of the corresponding relations increase linearly with inverse mean cubic side lengths  $1/d$  consistent with eq 2. The same plot is redrawn in Figure 3b, but now for  $D^{-1}$  against the particle number concentration  $(N_p)/(V_{\text{oil}})$ , realizing that the mass per particle  $m_p \approx \rho_p d^3$  and substitution in eq 2 yield  $D^{-1} = ((N_p d^2)/(6V_{\text{oil}} C))$ . Hence,  $D^{-1}$  should scale with  $d^2$  in this representation, which is confirmed by the manifest increase in slope steepness with particle size. These findings are compatible because larger particles have a high surface area per particle and fewer particles are necessary to stabilize emulsions with similar droplet sizes (Figure 3b). At the same time, larger cubes display a lower surface-to-volume ratio, and relatively higher particle weight concentrations are required to cover the same surface area. Although these plots were not corrected for sedimented particles, which are generally  $\leq 15\%$  of the added hematite microparticles, they display the expected linear trends in a qualitative way. Moreover, we also accounted for unadsorbed microparticles and corroborated the linear dependence of the average droplet diameter  $D$  with side length  $d$  more accurately, as shown in Figure 3c for 4 wt %.

**Packing and Orientation of Interfacial Cubes.** It is a fundamental challenge to maximize the coverage of the interface by particle adsorption and hence to reduce the

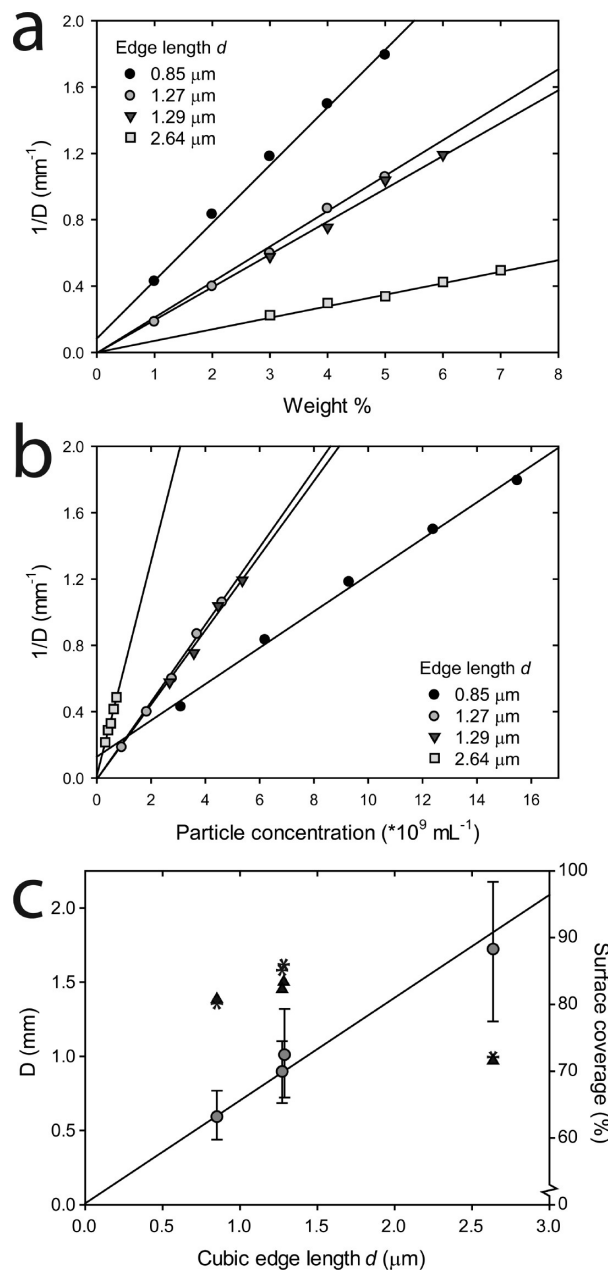


**Figure 3.** Inverse average oil droplet diameters  $1/D$  plotted against (a) wt % and (b) the particle concentration of stabilizing hematite microcubes. (c) Average oil droplet diameters  $D$  (○) and surface coverage determined from  $D$  (\*) and microscopic particle packings (▲) plotted against mean cubic side length  $d$  at 4 wt %.

major energy contribution opposing emulsion stability, the residual oil–water interface area, to a minimum. To achieve this, we employ cubic particles and investigate how close their arrangement approximates 100% interfacial coverage. Additionally, we study their orientation with respect to the interface. The stability of the emulsions and the size of the interfacial microparticles allow for *in situ* microscopy observations at the single-particle level. Figure 4 presents an overview of the microscopy data obtained for cubic hematite microparticles at the oil–water interface of decane droplets. The turbidity of the emulsion samples, however, obscures the clear visualization of emulsion droplets and attached particles. Therefore, emulsions were diluted with water which enabled detailed imaging of

emulsion droplets floating at the water–air interface. The integrity of the droplets was not affected by droplet transfer or evaporation. The spherical shape of the oil droplets is illustrated in Figure 4a. Upon changing the focal depth, different parts of the particle-covered interface can be imaged owing to the inherent curvature of the oil droplets, as shown for a small droplet in Figure 4b. Hence, consistent with the concept of adsorbed solid particles providing a barrier against droplet coalescence, optical imaging confirms particle coverage all over the droplet’s surface. The limited coalescence process is often rationalized by the assumption that only a single layer of colloids adsorbs at the oil–water interface. Our observations confirm the presence of a monolayer of microparticles stabilizing the emulsions.

The arrangement of the cubes that extends over the complete interface is displayed in Figure 4b–f. Hematite cubes are confined to assembly in two dimensions and are organized in dense monolayers with domains that display a packing intermediate between cubic and hexagonal, in a so-called  $\Lambda_0$  or  $\Lambda_1$  lattice.<sup>42</sup> The observed arrangement corresponds to the shape of the cubes exhibiting rounded edges: their shape is intermediate between a sphere, which favors hexagonal packing, and a perfect cube, which favors cubic packing. The order is more local as compared to perfect hexagonally packed or cubic close-packed structures. Because of their intermediate shape and flexibility in packing, particle defects are difficult to identify. In contrast, crystals from spheres contain characteristic point and line defects that indicate crystal grain boundaries. For small droplets, defects become more apparent as the curvature becomes an important factor constraining the packing (Figure 4b). The fact that ordered domains can be indicated implies a high interfacial coverage by the microparticles (Figure 4c–f). Theoretically, the densest surface packing for perfect cubes is 100%. For our rounded-edged cubes, superellipsoids with  $m$  between 3.5 and 4, the maximum 2D packing density varies between 94 and 95% for  $\Lambda_0$ - and  $\Lambda_1$ -lattice packings.<sup>42</sup> This is a higher coverage than can be realized for spheres (90.7%). Surface coverages were determined macroscopically from average emulsion droplet diameters  $D$  and from microscopic microparticle packings (Figure 3c). Generally, the surface coverage varied between 80 and 90% for cubes with different sizes. Interestingly, local domains were encountered with packing densities higher than theoretically possible for spheres.

In addition, the minimum areal fraction of the residual oil–water interface for the densest sphere packings is 9.3% for three-phase contact angles  $\theta_{ow}$  of exactly 90° and is very sensitive to  $\theta_{ow}$ . This results in much higher fractions of the particle-free interface in most situations. In contrast, the fraction of the oil–water interface that remains upon adsorption of the densest packing of cubes is lower than 9.3%, not for one specific contact angle but for a range of  $\theta_{ow}$  values. This is associated with the exclusive parallel orientation of the cubes, to be discussed in the following paragraphs. For cubes with  $d = 2.64 \mu\text{m}$ , the packing is somewhat lower (72%) and open spots are more frequently observed (Figure 4e), resulting in slightly smaller droplet sizes than expected. Figure 4f shows, however, that in the same sample some areas display higher packing densities. These observations may be related to the less cubic shape and slower dynamics of larger particles that may result in a suboptimal, jammed state.

We have also investigated the packing and orientation of particles at the oil–water interface with scanning electron

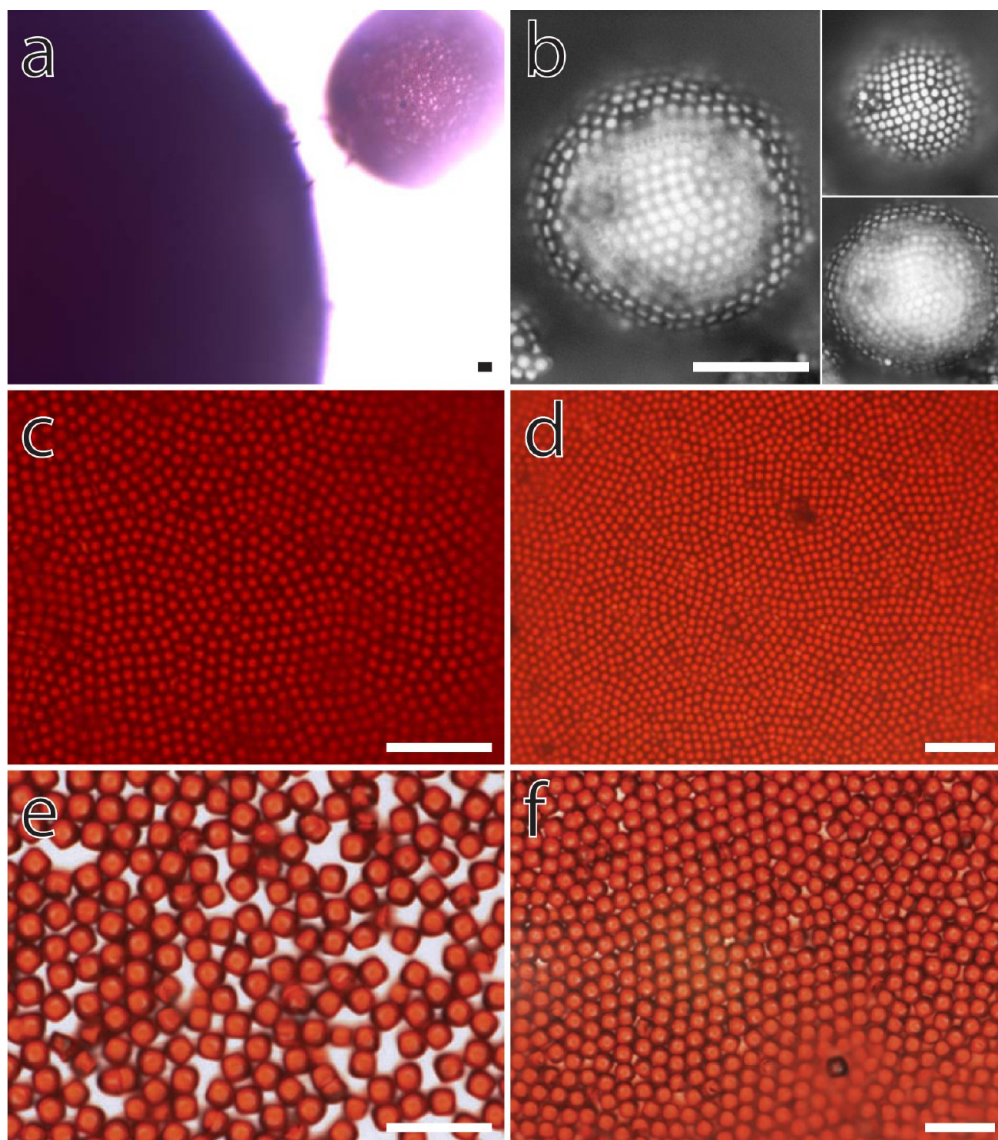


**Figure 4.** Optical microscopy images of emulsion droplets displaying the assembly and arrangement of cubic particles at the oil–water interface. The cubes have mean side lengths of (a–c) 1.27, (d) 1.29, and (e, f) 2.64  $\mu\text{m}$ . Scale bars are 10  $\mu\text{m}$ .

microscopy. To enable imaging, styrene emulsion droplets decorated with cubic microparticles were polymerized. Despite the solidification of the emulsion droplets, interfacial particle packings consistent with the optical microscopy observations were preserved, as shown in Figure 5a,b. Some interfacial regions, however, were free from particles. Although samples were carefully prepared for SEM imaging, particle release from polymerized droplets was inevitable and occurred even upon gentle droplet transfer. Upon close inspection of the electron micrographs, we observed characteristic dimples corresponding to imprints of previously attached cubes (e.g., see marked square in Figure 5b). In terms of applications, droplets densely covered by cubes could potentially give additional control of the permeability of so-called colloidosomes<sup>43</sup> because the particle-free interfacial spots are only small and narrow cavities between the face-to-face packed cubes need to be crossed.

We will now discuss the orientation of cubes residing at the oil–water interface. Interfacial particles have stable orientations if Young's law, which results in a three-phase contact angle  $\theta_{\text{ow}}$ , is satisfied all around the particle's surface. In contrast to

spherical particles, a number of recent studies revealed that  $\theta_{\text{ow}}$  for several anisotropic particles can remain constant only if the interface is distorted by undulations of the three-phase contact line.<sup>28,29,32–34</sup> As a consequence, the system wants to minimize these interfacial distortions, which give rise to long-range capillary interactions between the particles. However, indications for strong, long-range capillary interactions were not observed for cubes. We hypothesize that the cubic microparticles display a stable orientation upon adsorption without the need for significant interfacial deformations. Experiments on diluted monolayers at a macroscopic interface (SI Figure 2a) revealed that cubes were predominantly adsorbed as individual particles and clustering events that could indicate the presence of long-range capillary attractions were not detected. The only indirect observation that could potentially indicate the presence of capillary interactions is the jammed packing that is obtained only for very large cubes (Figure 4e), but we were unable to monitor the dynamics of interfacial adsorption. The exclusive orientation of the cubes at the oil–water interface is sketched in Figure 5c. All cubes are oriented with one of their flat sides

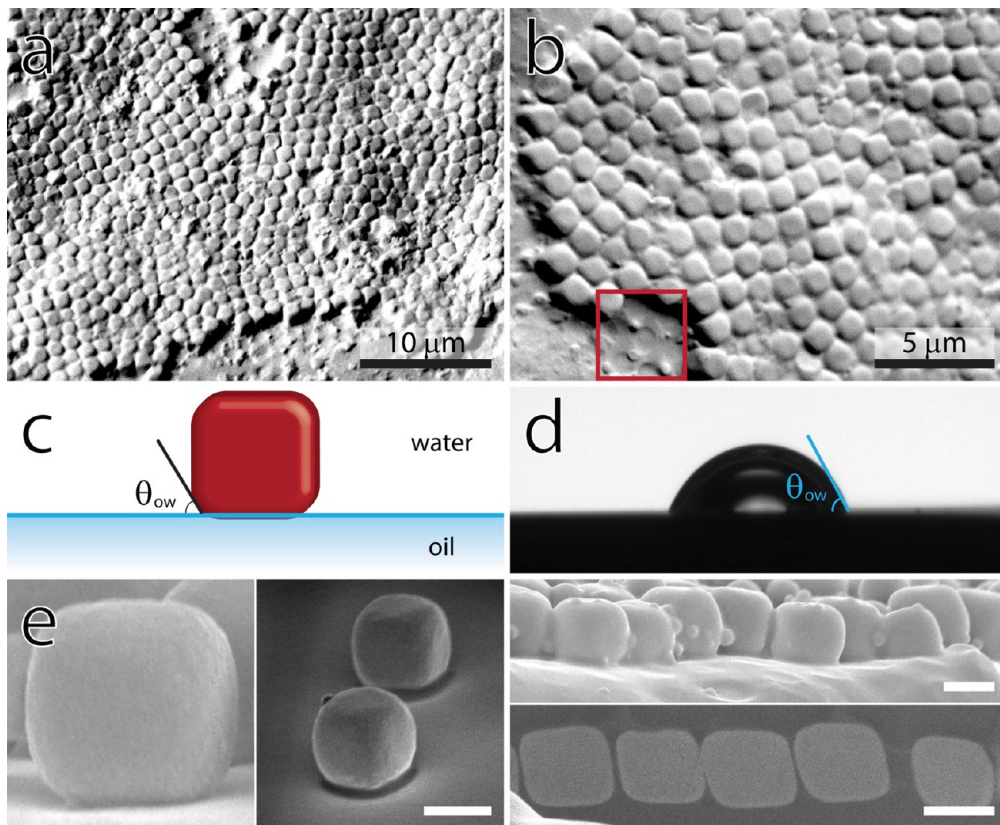


**Figure 5.** Arrangement and orientation of cubes ( $d = 1.27 \mu\text{m}$ ) at the interface of polymerized emulsion droplets, as visualized by scanning electron microscopy. (a, b) SEM pictures showing the arrangement of colloidal cubes. (c) Sketch of the parallel orientation of a cube attached to the oil–water interface. (d) Three-phase contact angle  $\theta_{\text{ow}}$  for a water droplet in styrene on a polished hematite surface. (e) SEM pictures confirm that cubes orient parallel with respect to the oil–water interface, with the majority of the cube surface exposed to the water phase. Scale bars are  $1 \mu\text{m}$ .

parallel to the oil–water interface. When viewed from the top in Figure 5a,b or the OM images in Figure 4, this is confirmed as one of the flat faces of the cube is observed. The rounded edges ensure that a wide range of values for  $\theta_{\text{ow}}$  can be satisfied all around the particle's surface in this parallel orientation while the interface remains flat. In fact, the particles can be regarded as cubes with curved edges and corners that determine their wetting behavior. The three-phase contact angle  $\theta_{\text{ow}}$  among oil, water, and hematite was  $75 \pm 7^\circ$  for styrene (Figure 5d). Similar values were obtained for decane ( $73 \pm 5^\circ$ ), hexadecane ( $73 \pm 6^\circ$ ), and isopropyl myristate ( $71 \pm 6^\circ$ ). Therefore, in all formulations oil-in-water emulsions were obtained. The majority of the cube's surface is exposed to the aqueous phase whereas one of the flat faces is immersed in the oil phase, which coincides with  $\theta_{\text{ow}} < 90^\circ$ . When viewed from the side, the parallel orientation of the cubes becomes even more clear (Figure 5e). For single particles, the parallel orientation of cubes is indeed thermodynamically most favorable, but stable tilted orientations are possible as well.<sup>44</sup> The observation of an exclusive parallel orientation and the absence of metastable, tilted orientations in our system may partially be a consequence of multiparticle effects such as capillary bridging, magnetic interactions, or van der Waals interactions between the large, flat faces. Our system features a complex interplay of different interactions on a curved liquid interface that was formed by the dynamic, nonequilibrium process of limited coalescence. To fully unravel the importance of the various interactions involved, a follow-up study is required using equilibrated

planar interfaces while varying the particle shapes and concentrations.

**Pickering Emulsions with Peanut-Shaped Microparticles.** The effect of particle anisotropy was further exploited by the use of peanut-shaped microparticles in the creation of Pickering emulsions. The addition of sulfate ions in the gel–sol method modifies the growth of microparticles via adsorption perpendicular to their (long)  $c$  axis.<sup>40</sup> In this way, we obtained peanut-shaped microparticles with an aspect ratio of 2.7 with small indentations perpendicular to the  $c$  axis of the particles (Figure 6a). Consistent with the limited coalescence process, emulsion droplet sizes were tunable and inversely linear with respect to particle concentration. Additionally, we prepared solid-stabilized emulsions by employing rounded-end ellipsoids (Supporting Information), distinct in shape and interfacial behavior from ellipsoids with sharp tips that were previously studied.<sup>27</sup>

Direct microscopic observations of peanut-covered emulsion droplets are displayed in Figure 6b,c. Because of the high particle coverage of the interface, approximately 79%, droplets remain intact for long times even when touching (Figure 6b). Peanuts assemble in particle stacks with their long axes parallel to each other (Figure 6c). Interestingly, the wide ends and indentations of the peanuts in those locally ordered stacks may interlock. There is, however, no clear correlation between orientations of different peanut stacks. Peanut-shaped particles were oriented with their long axes parallel to the oil–water interface, which was also confirmed by SEM observations (Figure 6d). In principle, Young's law can also be satisfied in a

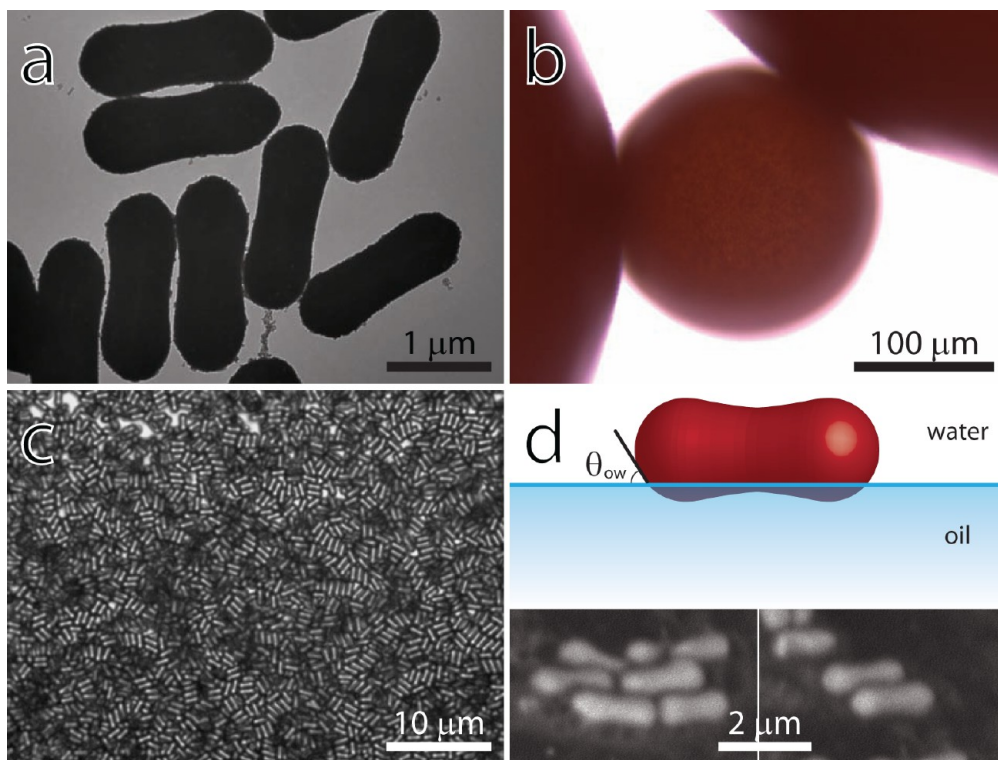


**Figure 6.** (a) Transmission electron micrograph of  $1.59 \pm 0.07 \mu\text{m} \times 0.59 \pm 0.03 \mu\text{m}$  peanut-shaped hematite microparticles. (b) Pickering emulsion droplets stabilized by peanut-shaped microparticles, as visualized by optical microscopy. (c) Peanuts assembled at the oil–water interface in interdigitating stacks. (d) Sketch and scanning electron micrographs of peanuts oriented parallel to their long axes with respect to the oil–water interface.

perpendicular orientation but is less favorable because of its lower energy gain upon adsorption. In agreement with their wetting characteristics ( $\theta_{\text{ow}} < 90^\circ$ ), peanuts were primarily exposed to the water phase. Despite their anisotropic particle shape, indications for long-range capillary attractions were not observed for interfacial peanuts in experiments on diluted monolayers (SI Figure 2b). The majority of the particles remained as individual particles at the interface, and clustering events due to capillary attractions were not observed. Their stable interfacial orientation is related to the gradual curvature gradient of the peanut shape. We propose that the three-phase contact angle can therefore be satisfied all around the particle surface without the need for significant interfacial deformations.

## CONCLUSIONS

We have investigated the effect of novel particle shapes in Pickering emulsions by employing cubic and peanut-shaped particles. These anisotropic microparticles display interfacial packings and orientations that were not studied before. Emulsions stabilized by monolayers of anisotropic hematite microparticles were formed via limited coalescence of particle-covered oil droplets. Droplets were stable against further coalescence for at least 1 year. With this study, we provide the first experimental realization of the limited coalescence of solid-stabilized emulsions with cubes, analogous to Wiley's seminal work in which an interfacial packing of cubes was assumed.<sup>19</sup> For instance, we verified a linear relationship between the emulsion droplet size and the side length  $d$  of interfacial cubes. The packing and orientation of anisotropic microparticles at the oil–water interface were studied with microscopy at the single-particle level. Cubes were assembled at the interface in

monolayers with a packing intermediate between hexagonal and cubic, with average densities of up to 90% and local densities higher than the densest sphere packings, reducing the energy penalty associated with the area of the residual oil–water interface to a minimum. Moreover, cubes were exclusively oriented parallel with one of their flat sides at the oil–water interface. Peanut-shaped microparticles organized locally in interdigitating stacks, oriented with their long axes parallel to the interface. Despite their anisotropic particle shape, indications for long-range capillary interactions were not observed for interfacial cubes and peanuts. The anisotropic particles display a stable orientation upon adsorption as a result of the rounded edges of the cubes and the moderate curvature of the peanuts, respectively. We propose that the three-phase contact angle can therefore be satisfied all around the particle surface without the need for significant interfacial deformations. To gain more knowledge of the importance of the various interactions involved and interfacial particle dynamics, a follow-up study is required that employs diluted monolayers of microparticles on a flat interface.

## ASSOCIATED CONTENT

### S Supporting Information

Derivation of limited coalescence for emulsion droplets stabilized by cubic particles, video of the formation of o/w emulsions stabilized by hematite cubes through limited coalescence, optical microscopy of diluted monolayers of cubes and peanuts at the macroscopic oil–water interface, and experimental data on Pickering emulsions with rounded-end ellipsoidal microparticles. This material is available free of charge via the Internet at <http://pubs.acs.org/>.

## AUTHOR INFORMATION

### Corresponding Author

\*E-mail: juliusdefolter@gmail.com; w.k.kegel@uu.nl.

### Notes

The authors declare no competing financial interest.

## ACKNOWLEDGMENTS

We thank Mathijs de Winter for (FIB-)SEM imaging, Chris Evers for help with styrene polymerization, and Jos van Rijssel for imaging the process of limited coalescence.

## REFERENCES

- (1) Ramsden, W. Separation of solids in the surface-layers of solutions and ‘suspensions’ (observations on surface-membranes, bubbles, emulsions, and mechanical coagulation). Preliminary account. *Proc. R. Soc. London* **1903**, *72*, 156–164.
- (2) Pickering, S. U. Emulsions. *J. Chem. Soc.* **1907**, *91*, 2001–2021.
- (3) Aveyard, R.; Binks, B. P.; Clint, J. H. Emulsions stabilised solely by colloidal particles. *Adv. Colloid Interface Sci.* **2003**, *100*, 503–546.
- (4) Binks, B. P.; Clint, J. H.; Mackenzie, G.; Simcock, C.; Whitby, C. P. Naturally occurring spore particles at planar fluid interfaces and in emulsions. *Langmuir* **2005**, *21*, 8161–8167.
- (5) Kalashnikova, I.; Bizot, H.; Cathala, B.; Capron, I. New Pickering emulsions stabilized by bacterial cellulose nanocrystals. *Langmuir* **2011**, *27*, 7471–7479.
- (6) de Folter, J. W. J.; van Ruijven, M. W. M.; Velikov, K. P. Oil-in-water Pickering emulsions stabilized by colloidal particles from the water-insoluble protein zein. *Soft Matter* **2012**, *8*, 6807–6815.
- (7) Binks, B. P.; Lumsdon, S. O. Pickering emulsions stabilized by monodisperse latex particles: effects of particle size. *Langmuir* **2001**, *17*, 4540–4547.
- (8) Binks, B. P.; Lumsdon, S. O. Influence of particle wettability on the type and stability of surfactant-free emulsions. *Langmuir* **2000**, *16*, 8622–8631.
- (9) Sacanna, S.; Kegel, W. K.; Philipse, A. P. Thermodynamically stable Pickering emulsions. *Phys. Rev. Lett.* **2007**, *98*, 158301.
- (10) Kraft, D. J.; de Folter, J. W. J.; Luigjes, B.; Castillo, S. I. R.; Sacanna, S.; Philipse, A. P.; Kegel, W. K. Conditions for equilibrium solid-stabilized emulsions. *J. Phys. Chem. B* **2010**, *114*, 10347–10356.
- (11) Kraft, D. J.; Luigjes, B.; de Folter, J. W. J.; Philipse, A. P.; Kegel, W. K. Evolution of equilibrium pickering emulsions—a matter of time scales. *J. Phys. Chem. B* **2010**, *114*, 12257–12263.
- (12) Fujii, S.; Read, E. S.; Binks, B. P.; Armes, S. P. Stimulus-responsive emulsifiers based on nanocomposite microgel particles. *Adv. Mater.* **2005**, *17*, 1014–1018.
- (13) Fujii, S.; Armes, S. P.; Binks, B. P.; Murakami, R. Stimulus-responsive particulate emulsifiers based on lightly cross-linked poly(4-vinylpyridine)-silica nanocomposite microgels. *Langmuir* **2006**, *22*, 6818–6825.
- (14) Gautier, F.; Destribats, M.; Perrier-Cornet, R.; Dechezelles, J. F.; Giermanska, J.; Heroguez, V.; Ravaine, S.; Leal-Calderon, F.; Schmitt, V. Pickering emulsions with stimulable particles: from highly- to weakly-covered interfaces. *Phys. Chem. Chem. Phys.* **2007**, *9*, 6455–6462.
- (15) Destribats, M.; Schmitt, V.; Backov, R. Thermostimulable Wax@SiO<sub>2</sub> core-shell particles. *Langmuir* **2010**, *26*, 1734–1742.
- (16) Destribats, M.; Lapeyre, V.; Sellier, E.; Lea-Calderon, F.; Ravaine, V.; Schmitt, V. Origin and control of adhesion between emulsion drops stabilized by thermally sensitive soft colloidal particles. *Langmuir* **2012**, *28*, 3744–3755.
- (17) Melle, S.; Lask, M.; Fuller, G. G. Pickering emulsions with controllable stability. *Langmuir* **2005**, *21*, 2158–2162.
- (18) Hardy, W. B. *Colloid Symp. Monogr.* **1928**, *16*, 8.
- (19) Wiley, R. M. Limited coalescence of oil droplets in coarse oil-in-water emulsions. *J. Colloid Sci.* **1954**, *9*, 427–437.
- (20) Whitesides, T. H.; Ross, D. S. Experimental and theoretical analysis of the limited coalescence process: stepwise limited coalescence. *J. Colloid Interface Sci.* **1995**, *169*, 48–59.
- (21) Arditty, S.; Whitby, C. P.; Binks, B. P.; Schmitt, V.; Leal-Calderon, F. Some general features of limited coalescence in solid-stabilized emulsions. *Eur. Phys. J. E* **2003**, *11*, 273–281.
- (22) Abend, S.; Bonnke, N.; Gutschner, U.; Lagaly, G. Stabilization of emulsions by heterocoagulation of clay minerals and layered double hydroxides. *Colloid Polym. Sci.* **1998**, *276*, 730–737.
- (23) Ashby, N. P.; Binks, B. P. Pickering emulsions stabilised by laponite clay particles. *Phys. Chem. Chem. Phys.* **2000**, *2*, 5640–5646.
- (24) Alargova, R. G.; Warhadpande, D. S.; Paunov, V. N.; Velev, O. D. Foam superstabilization by polymer microrods. *Langmuir* **2004**, *20*, 10371–10374.
- (25) Kim, J.; Cote, L. J.; Kim, F.; Yuan, W.; Shull, K. R.; Huang, J. X. Graphene oxide sheets at interfaces. *J. Am. Chem. Soc.* **2010**, *132*, 8180–8186.
- (26) Bowden, N.; Terfort, A.; Carbeck, J.; Whitesides, G. M. Self-assembly of mesoscale objects into ordered two-dimensional arrays. *Science* **1997**, *276*, 233–235.
- (27) Madivala, B.; Vandebril, S.; Fransaer, J.; Vermant, J. Exploiting particle shape in solid stabilized emulsions. *Soft Matter* **2009**, *5*, 1717–1727.
- (28) Loudet, J. C.; Alsayed, A. M.; Zhang, J.; Yodh, A. G. Capillary interactions between anisotropic colloidal particles. *Phys. Rev. Lett.* **2005**, *94*, 018301.
- (29) Loudet, J. C.; Yodh, A. G.; Pouliquen, B. Wetting and contact lines of micrometer-sized ellipsoids. *Phys. Rev. Lett.* **2006**, *97*, 018304.
- (30) Madivala, B.; Fransaer, J.; Vermant, J. Self-assembly and rheology of ellipsoidal particles at interfaces. *Langmuir* **2009**, *25*, 2718–2728.
- (31) Loudet, J. C.; Pouliquen, B. How do mosquito eggs self-assemble on the water surface? *Eur. Phys. J. E* **2011**, *34*, 76.
- (32) Yunker, P. J.; Still, T.; Lohr, M. A.; Yodh, A. G. Suppression of the coffee-ring effect by shape-dependent capillary interactions. *Nature* **2011**, *476*, 308–311.
- (33) Lewandowski, E. P.; Bernate, J. A.; Tseng, A.; Searson, P. C.; Stebe, K. J. Oriented assembly of anisotropic particles by capillary interactions. *Soft Matter* **2009**, *5*, 886–890.
- (34) Lewandowski, E. P.; Cavallaro, M.; Botto, L.; Bernate, J. C.; Garbin, V.; Stebe, K. J. Orientation and self-assembly of cylindrical particles by anisotropic capillary interactions. *Langmuir* **2010**, *26*, 15142–15154.
- (35) Sugimoto, T.; Sakata, K. Preparation of monodisperse pseudocubic  $\alpha$ -Fe<sub>2</sub>O<sub>3</sub> particles from condensed ferric hydroxide gel. *J. Colloid Interface Sci.* **1992**, *152*, 587–590.
- (36) Sugimoto, T.; Sakata, K.; Muramatsu, A. Formation mechanism of monodisperse pseudocubic  $\alpha$ -Fe<sub>2</sub>O<sub>3</sub> particles from condensed ferric hydroxide gel. *J. Colloid Interface Sci.* **1993**, *159*, 372–382.
- (37) Rossi, L.; Sacanna, S.; Irvine, W. T. M.; Chaikin, P. M.; Pine, D. J.; Philipse, A. P. Cubic crystals from cubic colloids. *Soft Matter* **2011**, *7*, 4139–4142.
- (38) Meijer, J. M.; Hagemans, F.; Rossi, L.; Byelov, D. V.; Castillo, S. I. R.; Snigirev, A.; Snigireva, I.; Philipse, A. P.; Petukhov, A. V. Self-assembly of colloidal cubes via vertical deposition. *Langmuir* **2012**, *28*, 7631–7638.
- (39) Sugimoto, T.; Khan, M. M.; Muramatsu, A. Preparation of monodisperse peanut-type  $\alpha$ -Fe<sub>2</sub>O<sub>3</sub> particles from condensed ferric hydroxide gel. *Colloids Surf., A* **1993**, *70*, 167–169.
- (40) Sugimoto, T.; Wang, Y. S. Mechanism of the shape and structure control of monodispersed  $\alpha$ -Fe<sub>2</sub>O<sub>3</sub> particles by sulfate ions. *J. Colloid Interface Sci.* **1998**, *207*, 137–149.
- (41) Delaney, G. W.; Cleary, P. W. The packing properties of superellipsoids. *Europhys. Lett.* **2010**, *89*, 34002.
- (42) Jiao, Y.; Stillinger, F. H.; Torquato, S. Optimal packings of superdisks and the role of symmetry. *Phys. Rev. Lett.* **2008**, *100*, 245504.
- (43) Dinsmore, A. D.; Hsu, M. F.; Nikolaides, M. G.; Marquez, M.; Bausch, A. R.; Weitz, D. A. Colloidosomes: selectively permeable

capsules composed of colloidal particles. *Science* **2002**, *298*, 1006–1009.

(44) Morgan, A. R.; Ballard, N.; Rochford, L. A.; Nurumbetov, G.; Skelhon, T. S.; Bon, S. A. F. Understanding the multiple orientations of isolated superellipsoidal hematite particles at the oil-water interface. *Soft Matter* **2013**, *9*, 487–491.